# Variable Coherence Scattering Microscopy

Erwan Baleine and Aristide Dogariu

*College of Optics and Photonics: CREOL and FPCE, University of Central Florida, Orlando, Florida 32816, USA*

(Received 28 July 2005; published 3 November 2005)

We propose and demonstrate the feasibility of a new microscopic technique, which is based on variable coherence illumination. By manipulating the spatial coherence properties of an incident evanescent field, subwavelength resolution is achieved over a large field of view from far-field intensity measurements.

DOI: 10.1103/PhysRevLett.95.193904 PACS numbers: 42.25.−p, 42.30.Wb

Optical techniques for imaging and structural characterization are widespread. Conventional imaging techniques rely on propagating fields and, therefore, their spatial resolution is limited by the radiation's wavelength. Recent advances in near-field optics have led to the development of many microscopy techniques for achieving imaging with a spatial resolution beyond the classical diffraction limit. Atomic-force microscopy, near-field scanning optical microscopy [1], and photon scanning tunneling microscopy [2] have been successful in recovering images of subwavelength objects. However, this improved resolution comes at the expense of the most appealing characteristic of optical imaging, namely, its parallel processing capability. Because a scanning probe operation is required to build up the image point by point, the approach is time consuming and, moreover, it is practically restricted to imaging of very small areas.

There are many situations of practical interest where conventional imaging is irrelevant and only a statistical description of the medium under scrutiny is meaningful. In this case, light scattering approaches are used to determine the structural properties of heterogeneous media as described by statistical descriptors such as the correlation of its scattering potential.

Second order statistics of optical properties are indeed of considerable interest, especially in determining structural information about objects such as large nanostructure arrays. Correlation measurements on monolayers of biological cells have been recently performed demonstrating the increased medical interest in investigating the morphology of subcellular structures as well as long range correlations between cells [3]. In this last experiment, the proposed method was, however, model dependant and could hardly be applied to arbitrary scattering objects. Nevertheless, the development of nondestructive microscopic techniques is of primary interest for characterizing biological media. In this context, it is worth mentioning that total internal reflection tomography [4] is an interesting approach which, however, requires challenging measurements of the optical fields. An alternative method [5] based on power extinction measurements has been proposed but not demonstrated.

In this Letter, we introduce and demonstrate the principle of variable coherence scattering microscopy (VCSM). In this approach, the object under test is probed by an evanescent field which has its spatial coherence properties adjustable at subwavelength scales. Our results are remarkable in the sense that subwavelength resolution is achieved from simple far zone intensity measurements. Notably, the technique we are illustrating here can be implemented without any moving parts for both illuminating the sample and detecting the scattered light.

Let us consider a quasimonochromatic partially coherent field with central frequency $\omega$ which is incident upon a dielectric medium occupying a finite domain $D$ and described by the complex susceptibility $\eta(\mathbf{r}, \omega)$, where $\mathbf{r}$ is the position vector in space. The second order fluctuations of this field can be described statistically by the cross-spectral density $W^{(i)}(\mathbf{r}_1, \mathbf{r}_2) = \langle U^{(i)*}(\mathbf{r}_1) U^{(i)}(\mathbf{r}_2) \rangle_U$ where the averaging $\langle \ldots \rangle_U$ is taken over the stationary ensemble $\{U^{(i)}(\mathbf{r}) \exp(-i\omega t)\}$ of monochromatic realizations. For simplicity, in the following we will ignore any polarization effects and consider just the scalar situation. For subwavelength structures and optically thin media it is appropriate to regard the scattering as being weak and therefore the first-order Born approximation can be used. In these conditions, the intensity scattered in the direction $\mathbf{k}_s$ is [6]

$$I^{(s)}(\mathbf{k}_s) = \frac{k_0^2}{r^2} \iint_D C(\mathbf{r}_1, \mathbf{r}_2) W^{(i)}(\mathbf{r}_i, \mathbf{r}_2) \times \exp[i\mathbf{k}_s \cdot (\mathbf{r}_1 - \mathbf{r}_2)] d^3\mathbf{r}_1 d^3\mathbf{r}_2, \quad (1)$$

where $C(\mathbf{r}_1, \mathbf{r}_2) = \langle \eta^*(\mathbf{r}_1) \eta(\mathbf{r}_2) \rangle_\eta$ is the averaged spatial correlation of the complex susceptibility $\eta(\mathbf{r})$ and $k_0 = \omega/c$ is the wave number.

Diffraction tomography is conventionally used to obtain $C$ from measurements of the cross-spectral density of the scattered field in two different planes [7]. Because the dimensionality of the measured cross-spectral density is smaller than that of $C$, the problem was shown to be, in general, undetermined unless the random object is quasihomogeneous. Even in these conditions, the measurement procedure is quite challenging since the detection system needs access to a wide range of scattering angles in order to provide sufficient data for a robust inversion process [8].

Inspecting further Eq. (1), one can immediately observe that another possibility exists to obtain the correlation function $C$. Instead of determining the scattered intensity at different angles, one can measure the intensity scattered

 

in a single direction while varying the coherence properties of the incident field which are described by $W^{(i)}$. This represents the basis of the variable coherence tomography technique. Recently, we have demonstrated that the degree of spatial correlation of a quasihomogeneous scattering medium can be retrieved from simple intensity measurements [9]. The resolution of the reconstruction was limited by the size of the coherence volume, whose dimensions can exceed many wavelengths in the case of a propagating beamlike field. Exploiting the high frequency content of evanescent waves, a spatial resolution beyond the diffraction limit can be achieved [4]. In the newly proposed method, an ensemble of evanescent waves are incoherently superposed in order to generate a field of speckles smaller than the wavelength. Moreover, in this field, the correlation properties can be adjusted between speckles separated by distances as large as several tens of wavelengths.

Let us consider an incoherent superposition of evanescent plane waves defined by their complex wave vectors $\mathbf{k} = (\mathbf{q}, i\gamma)$ where $\mathbf{q}$ is the transverse part and $\gamma = \sqrt{\mathbf{q}^2 - k_0^2}$. Evanescent waves are generated at the interface $(x, y, z = 0)$ between air $(z \geq 0)$ and a dielectric medium $(z < 0)$ with a refractive index $n$. Consequently, the modulus of the transverse wave vector $\mathbf{q}$ is confined to the region $\mathbf{\Gamma}$ defined by $k_0 \leq |\mathbf{q}| \leq nk_0$. Let us further consider that the intensity of the evanescent field is modulated in the $\mathbf{k}$ domain so that the plane wave defined by the transverse wave vector $\mathbf{q}$ has the intensity

$$I_e(\mathbf{q}) = \tfrac{1}{2}Q(\mathbf{q})(1 + m\cos[\mathbf{q}\cdot\mathbf{\Delta}\rho_0 - \phi]), \tag{2}$$

where $m$ is a modulation factor taking values between 0 and 1, and $Q(\mathbf{q})$ is positive if $\mathbf{q} \in \mathbf{\Gamma}$ and equals zero otherwise. The periodicity of the intensity modulation is adjusted by the value of the vector $\mathbf{\Delta}\rho_0$, while the phase $\phi$ is determined by the condition $\mathbf{q}\cdot\mathbf{\Delta}\rho_0 = 0$.

One can show that the incoherent superposition of evanescent plane waves with intensity $I_e(\mathbf{q})$ given by Eq. (2) generates a partially coherent evanescent field with a cross-spectral density of the form [10]

$$W^{(i)}(\mathbf{r}_1, \mathbf{r}_2) = \chi(\mathbf{\Delta}\rho, z_1, z_2) + \frac{m}{2}\exp[-i\phi]\chi(\mathbf{\Delta}\rho - \mathbf{\Delta}\rho_0, z_1, z_2) + \frac{m}{2}\exp[i\phi]\chi(\mathbf{\Delta}\rho + \mathbf{\Delta}\rho_0, z_1, z_2), \tag{3}$$

where $z_1$ and $z_2$ are the projections of $\mathbf{r}_1$ and $\mathbf{r}_2$ along the $z$ axis, and $\mathbf{\Delta}\rho = \mathbf{r}_{\perp 1} - \mathbf{r}_{\perp 2}$ with $\mathbf{r}_\perp$ being the projection of $\mathbf{r}$ onto the $(x, y)$ plane. When $m$ equals zero in Eq. (2), the incident field is spatially coherent in a volume defined by the function $\chi$:

$$\chi(\mathbf{\Delta}\rho, z_1, z_2) = \frac{1}{2}\iint_{-\infty}^{\infty} Q(\mathbf{q})\exp[-\gamma(z_1 + z_2)] \times \exp[-i\mathbf{q}\cdot\mathbf{\Delta}\rho]d^2\mathbf{q}. \tag{4}$$

The cross-spectral density $W^{(i)}$ of the evanescent field in the plane of the interface $z = 0$ is illustrated in Fig. 1. When the intensity $I_e(\mathbf{q})$ is modulated, i.e., when $m$ is greater than zero, a secondary peak of coherence arises at a position $\mathbf{\Delta}\rho_0$ from the main coherence peak centered at $\mathbf{\Delta}\rho = \mathbf{0}$. The separation $\mathbf{\Delta}\rho_0$ can be continuously adjusted by varying the intensity $I_e(\mathbf{q})$. The incident field induces coherent scattering from regions in the medium which are separated by a distance of several wavelengths corresponding to the norm $|\mathbf{\Delta}\rho_0|$. Because of the evanescent nature of the incident field, only the high frequency components of the complex susceptibility corresponding to subwavelength features are excited during the scattering process.

From Eq. (3), one can see that $W^{(i)}(\mathbf{r}_1, \mathbf{r}_2)$ depends only on the transverse separation $\mathbf{\Delta}\rho = \mathbf{r}_{\perp 1} - \mathbf{r}_{\perp 2}$. It is therefore relevant to consider a quasihomogeneous medium [7] with transversely invariant statistical properties, namely $C(\mathbf{r}_1, \mathbf{r}_2) = A[(\mathbf{r}_{\perp 1} + \mathbf{r}_{\perp 2})/2] \times \mu(\mathbf{\Delta}\rho, z_1, z_2)$ where $\mu$ is the degree of spatial correlation of the complex susceptibility and $A(\mathbf{r}_\perp) = C(\mathbf{r}_\perp, \mathbf{r}_\perp)$ is the second moment of $C$ in the plane $z = 0$. The function $A(\mathbf{r}_\perp)$ is assumed to vary more slowly with $\mathbf{r}_\perp$ than the variation of $\mu(\mathbf{\Delta}\rho, z_1, z_2)$ with $\mathbf{\Delta}\rho$. From Eqs. (1) and (3), it follows that the scattered intensity depends on $\mathbf{\Delta}\rho_0$ as

$$I^{(s)}(\mathbf{k}_s, \mathbf{\Delta}\rho_0) = G(\mathbf{k}_s, \mathbf{0}) + m|G(\mathbf{k}_s, \mathbf{\Delta}\rho_0)|\cos(\Psi), \tag{5}$$

with $\Psi = \mathbf{k}_{s\perp}\cdot\Delta\rho_o - \phi + \phi_G(\mathbf{k}_s, \Delta\rho)$ and $\phi_G(\mathbf{k}_s, \Delta\rho_0)$ being the argument of the function $G(\mathbf{k}_s, \mathbf{\Delta}\rho_0)$ defined as

$$G(\mathbf{k}_s, \mathbf{\Delta}\rho_0) = \frac{k_0^2}{r^2}A_0\iint_{-\infty}^{\infty}\int_0^{z_m}\mu(\mathbf{\Delta}\rho - \mathbf{\Delta}\rho_0, z_1, z_2)\chi(\mathbf{\Delta}\rho, z_1, z_2)\exp[i\mathbf{k}_{s\perp}\cdot\mathbf{\Delta}\rho + ik_{sz}(z_1 - z_2)]d^2\mathbf{\Delta}\rho dz_1 dz_2. \tag{6}$$

In Eq. (6), $z_m$ is the longitudinal extend of the medium. The integration over $\mathbf{\Delta}\rho$ can be extended to infinity because, in practice, the transverse dimensions of the object are much larger than both the transverse width of $\chi(\mathbf{\Delta}\rho, z_1, z_2)$ and the range of values taken by $|\mathbf{\Delta}\rho|$ for which $\mu(\mathbf{\Delta}\rho, z_1, z_2)$ is nonzero. The proportionality factor $A_0$ is defined as $A_0 = \int A(\mathbf{r}_\perp)d^2\mathbf{r}_\perp$ and is proportional to the transverse area of the object if $A$ is constant.

Equation (5) along with Eq. (6) constitutes the basis of the variable coherence scattering microscopy. As the coherence properties of the illuminating evanescent field are varied, the scattered intensity in any given direction fluctuates accordingly to the correlation properties of the medium. Conventional envelope and phase reconstruction can be used to recover $G$ and to infer information about the degree of spatial correlation $\mu$. Although a complete inversion of Eq. (6) requires *a priori* knowledge about the $z$ dependence of $\mu$, some practical situations could lead to a simpler expression of Eq. (6), which can be readily inverted. This is indeed the case if $\mu$ is independent of $z$ or if the sample is much thinner than the wavelength and no correlation along the $z$ direction can be assumed. However,

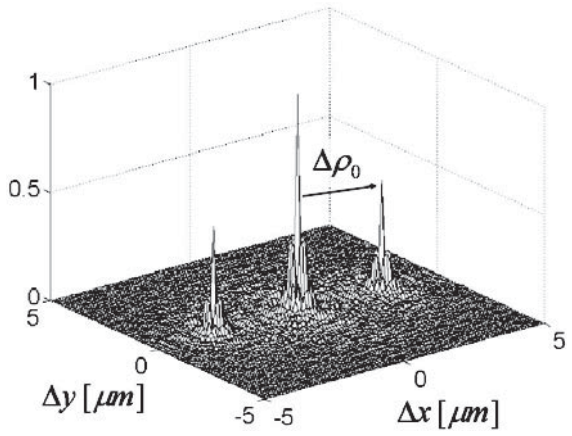


FIG. 1. Normalized cross-spectral density of the evanescent field as evaluated from Eq. (4) for $z_1 = z_2 = 0$, $Q(\mathbf{q}) = 1$, and $k_0 \leq |\mathbf{q}| \leq nk_0$.

even in the general case, structural information about the sample can be obtained from the expression of $G$ as we will see in the following.

To demonstrate the feasibility of the inversion procedure, a proof-of concept experiment has been conducted. The spherical geometry shown in Fig. 2 was used to generate evanescent waves with transverse wave vectors $\mathbf{q} \in \mathbf{\Gamma}$. The light emitted by a hemispherical secondary source $H$ is collected by a hemisphere prism $L$ concentric with $H$. The dimensions of $H$ and $L$ are such that the surface of the source lies in the focal surface of the prism. The radius and the index of refraction of $L$ are, respectively, $R_L = 21.5$ mm and $n = 1.78$. The intensity distribution across the source is modulated according to Eq. (2). Consequently, the light originating from a point on the source $H$ generates an evanescent plane wave at the planar interface $(x, y)$ of the prism. Spatial incoherence of the source is obtained by slightly vibrating $H$ while recording the intensity.

An interferometer operating at $\lambda = 532$ nm was used to generate a fringe pattern with adjustable periodicity which was projected onto a hemispherical diffuser used as a secondary source. The light scattered by the sample in the $z$ direction, i.e., $\mathbf{k}_{s\perp} = \mathbf{0}$, is collected by a multimode

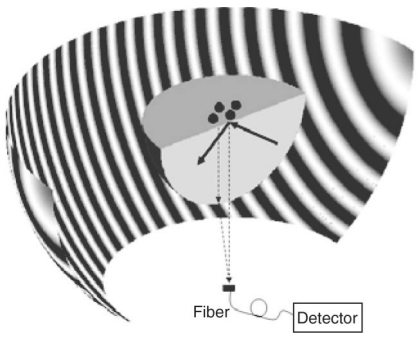


FIG. 2. Schematic of the setup used to generate evanescent waves with transverse wave vectors $k_0 \leq |\mathbf{q}| \leq nk_0$.

fiber located in the focal plane of a 10× microscope objective. The objective was placed above the object for convenience but the detection could have been done as well from below as represented in Fig. 2. The diameter of the field of view seen by the fiber was around 1 mm.

The scattering system exemplified here is a monolayer of polystyrene microspheres of diameter $d = 0.97$ $\mu$m and index of refraction $n_s = 1.59$. Using conventional analysis of several microscope images of the sample, we estimated the packing fraction to be $f = 0.7$. The angular light scattered from such a monolayer of spheres is well described in the single scattering approximation [11] and it can be expressed as the product between the single particle phase function $P$ and the structure factor $S$ describing the spheres' arrangement in the monolayer. We denote as $I^{(m)}(\mathbf{k}_{sz}, \mathbf{q}) = P(\mathbf{k}_{sz}, \mathbf{k})S(\mathbf{q})Q(\mathbf{q})$ the intensity scattered in the direction $z$ by the monolayer illuminated by an evanescent waves with wave vector $\mathbf{k} = (\mathbf{q}, i\gamma)$ and intensity $Q(\mathbf{q})$. The expression for the scattered intensity in Eq. (1) establishes the following relationship between $I^{(m)}$ and an effective spatial correlation function $C$ describing the medium:

$$I^{(m)}(\mathbf{k}_{sz}, \mathbf{q}) = \frac{k_0^2}{r^2} \iint_D C(\mathbf{r}_1, \mathbf{r}_2) W_p^{(i)}(\mathbf{r}_1, \mathbf{r}_2) \times \exp[ik_{sz}(z_1 - z_2)] d^3\mathbf{r}_1 d^3\mathbf{r}_2. \quad (7)$$

In formula (7), $W_p^{(i)}(\mathbf{r}_1, \mathbf{r}_2) = Q(\mathbf{q}) \exp[-i\mathbf{q} \cdot (\mathbf{r}_{\perp 1} - \mathbf{r}_{\perp 2})] \exp[-(z_1 + z_2)\gamma]$ represents the cross-spectral density of an evanescent plane wave with incident wave vector $\mathbf{k} = (\mathbf{q}, i\gamma)$ and intensity $Q(\mathbf{q})$. Using Eqs. (4), (6), and (7) and the expression for $W_p^{(i)}$, the function $G(\mathbf{k}_{sz}, \Delta\rho_0)$ can be regarded as the Fourier transform of $I^{(m)}(\mathbf{k}_{sz}, \mathbf{q})$ with respect to $\mathbf{q}$, namely $G(\mathbf{k}_{sz}, \mathbf{\Delta}\rho_0) = \int_{-\infty}^{\infty} I^{(m)}(\mathbf{k}_{sz}, \mathbf{q}) \times \exp(-i\mathbf{q} \cdot \mathbf{\Delta}\rho_0) d^2\mathbf{q}$. Being proportional to $Q(\mathbf{q})$, $I^{(m)}(\mathbf{k}_{sz}, \mathbf{q})$ vanishes for $\mathbf{q} \notin \mathbf{\Gamma}$. Moreover, since the function $I^{(m)}(\mathbf{k}_{sz}, \mathbf{q})$ is real and even with respect to $\mathbf{q}$, $G(\mathbf{k}_{sz}, \mathbf{\Delta}\rho_0)$ is real and, using Eq. (5), the intensity $I^{(s)}(\mathbf{k}_{sz}, \mathbf{\Delta}\rho_0)$ scattered in the $z$ direction becomes

$$I^{(s)}(\mathbf{k}_{sz}, \mathbf{\Delta}\rho_0) = G(\mathbf{k}_{sz}, \mathbf{0}) + mG(\mathbf{k}_{sz}, \mathbf{\Delta}\rho_0)\cos(\phi). \quad (8)$$

It follows that $I^{(m)}(\mathbf{k}_{sz}, \mathbf{q})$ can be determined by Fourier transforming $G(\mathbf{k}_{sz}, \mathbf{\Delta}\rho_0)$ obtained from the intensity data $I^{(s)}(\mathbf{k}_{sz}, \mathbf{\Delta}\rho_0)$. Since $I^{(m)}(\mathbf{k}_{sz}, \mathbf{q})$ depends only on the modulus $|\mathbf{q}|$, the procedure is further simplified using a Hankel transform of zero order and the inversion formula becomes

$$I^{(m)}(\mathbf{k}_{sz}, \mathbf{q}) = \frac{1}{m\cos(\phi)} \int_0^{\infty} [I^{(s)}(\mathbf{k}_{sz}, \Delta\rho_0) - G(\mathbf{k}_{sz}, \mathbf{0})] \times J_0(q\Delta\rho_0)\Delta\rho_0 d\Delta\rho_0, \quad (9)$$

where $G(\mathbf{k}_{sz}, \mathbf{0})$ is the value of the scattered intensity for large $\Delta\rho_0$ where the function $G(\mathbf{k}_{sz}, \mathbf{\Delta}\rho_0)$ is assumed to vanish.

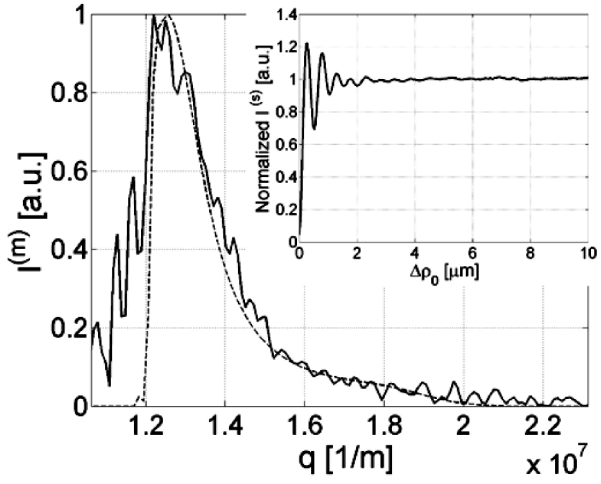


FIG. 3. High spatial frequency content of the intensity $I^{(m)}(\mathbf{k}_{sz}, \mathbf{q})$ scattered by a monolayer of 0.97 $\mu$m diameter particles. The solid line represents the results of the Hankel transform of the measured intensity $I^{(s)}(\mathbf{k}_{sz}, \Delta\rho_0)$, whereas the dashed line corresponds to an analytical result obtained as explained in the text. The inset shows part of the normalized intensity $I^{(s)}(\mathbf{k}_{sz}, \Delta\rho_0)$ obtained experimentally for $0 \leq \Delta\rho_0 \leq 10$ $\mu$m.

$I^{(s)}(\mathbf{k}_{sz}, \Delta\rho_0)$ was experimentally measured for $\Delta\rho_0$ ranging from 0 to 30 $\mu$m and $I^{(m)}(\mathbf{k}_{sz}, \mathbf{q})$ was obtained as a the result of a Hankel transform according to Eq. (9). The result of this procedure is presented in Fig. 3 for $q$ ranging from $k_0 = 11.8\ \mathrm{nm}^{-1}$ to $nk_0 = 21\ \mathrm{nm}^{-1}$. Also shown as an inset is the normalized intensity $I^{(s)}$ obtained experimentally. In order to check the validity of the experimental data, a comparison was made with available analytical expressions for $P(\mathbf{k}_{sz}, \mathbf{k})$, $S(\mathbf{q})$, and $Q(\mathbf{q})$. The phase function $P$ was calculated in terms of partial wave expansion [5] for a sphere of diameter $d = 0.97$ $\mu$m and index of refraction $n_s = 1.59$. The structure factor $S$ was computed using the Percus-Yevick approximation for the system of hard disks with a packing fraction $f = 0.7$ [12]. Since the source $H$ emits light isotropically, the intensity $Q$ of the evanescent plane waves illuminating the sample is simply proportional to the corresponding Fresnel transmission coefficient for unpolarized light [13].

The good agreement between the experimental and analytical data shown in Fig. 3 clearly demonstrates that the high spatial frequency content of the scattered intensity can be retrieved using VCSM. Our technique is therefore sensitive to the structural properties of subwavelength features over an extended field of view, which, in our experiment, had a diameter of 1 mm but could, in principle, be even larger. Because the light scattered from the sample can be detected from either above or below the sample as shown in Fig. 2, VCSM can be easily integrated with other types of microscopy for capability.

In conclusion, we introduced the concept of a novel microscopy technique based on controlling the spatial coherence properties of the illuminating field at subwavelength scale. We have demonstrated that the high spatial frequency components of the sample can be reconstructed from simple far zone intensity measurements. Subwavelength resolution is obtained over a very large field of view without using a scanning probe. Contrary to standing-wave fluorescence imaging [14], VCSM does not require fluorophore tagging of biological specimens. We also note that the practical technique presented here is implemented without any moving parts which makes VCSM an ideal candidates for high throughput sensing and screening for various applications in biology and medicine.

Finally, we would like to emphasize that the concept of using spatial coherence properties of radiation in a tomographic procedure is applicable to other ranges of electromagnetic radiation. Moreover, our results are of general importance because they demonstrate a modality of solving an inverse problem based only on far-field intensity data while achieving a resolution better than the radiation's wavelength.

This work was partially supported by the Air Force Research Laboratory and the Florida Photonics Center of Excellence.

[1] E. Betzig and J. K. Trautman, Science **257**, 189 (1992).
[2] R. C. Reddick, R. J. Warnack, and T. L. Ferrel, Phys. Rev. B **39**, 767 (1989).
[3] Adam Wax, C. Yang, V. Backman, K. Badizadegan, C. W. Boone, R. R. Dasari, and M. S. Feld, Biophys. J. **82**, 2256 (2002).
[4] P. S. Carney and J. C. Schotland, Opt. Lett. **26**, 1072 (2001).
[5] P. S. Carney, V. A. Markel, and J. C. Schotland, Phys. Rev. Lett. **86**, 5874 (2001).
[6] J. Jannson, T. Jannson, and E. Wolf, Opt. Lett. **13**, 1060 (1988).
[7] D. G. Fisher and E. Wolf, Opt. Commun. **133**, 17 (1997).
[8] E. Wolf, in *Trends in Optics*, edited by A. Consortini (Academic Press, San Diego, California, 1996), Vol. 3, pp. 83–110.
[9] E. Baleine and A. Dogariu, Opt. Lett. **29**, 1233 (2004).
[10] The field $U^{(i)}$ in the half space $z \geq 0$ can be expressed in terms of its angular spectrum of evanescent plane waves [see L. Mandel and E. Wolf, *Optical Coherence and Quantum Optics* (Cambridge University Press, Cambridge, 1995), Chap. 3, pp. 112–113]. The evaluation of $W^{(i)}$ involves a fourfold integral which reduces to a twofold one by considering uncorrelated plane waves in the $\mathbf{q}$ space. Inserting the intensity distribution given in Eq. (2) into this integral leads then to the form of Eq. (3).
[11] V. A. Loiko, V. P. Dick, and A. P. Ivanov, J. Opt. Soc. Am. A **17**, 2040 (2000).
[12] M. Baus and J. L. Colot, J. Phys. C **19**, L643 (1986).
[13] M. Born and E. Wolf, *Principle of Optics* (Cambridge University Press, Cambridge, England, 1999), Chap. 1, pp. 38–51.
[14] G. E. Cragg and P. T. C. So, Opt. Lett. **25**, 46 (2000).